Chinese Chemical Letters 34 (2023) 107814

Contents lists available at ScienceDirect

Chinese Chemical Letters

journal homepage: www.elsevier.com/locate/cclet

Non-3d metal modulated zinc imidazolate frameworks for CO_2 cycloaddition in simulated flue gas under ambient condition

Yan-Tong Xu[a,b,1], Zi-Ming Ye[a,1], De-Xuan Liu[a], Xiao-Yun Tian[a], Dong-Dong Zhou[a], Chun-Ting He[a,c,*], Xiao-Ming Chen[a,*]

[a] MOE Key Laboratory of Bioinorganic and Synthetic Chemistry, School of Chemistry, Sun Yat-Sen University, Guangzhou 510275, China
[b] Guangzhou Institute of Energy Conversion, Chinese Academy of Sciences, Guangzhou 510640, China
[c] MOE Key Laboratory of Fluorine and Silicon for Energy Materials and Chemistry, College of Chemistry and Chemical Engineering, Jiangxi Normal University, Nanchang 330022, China

ARTICLE INFO

Article history:
Received 29 July 2022
Revised 31 August 2022
Accepted 6 September 2022
Available online 11 September 2022

Keywords:
Non-3d metal modulation
Metal-organic framework
CO_2 fixation
Flue gas
Cycloaddition reaction

ABSTRACT

Cycloaddition of CO_2 and epoxide into cyclic carbonate is one of the most efficient ways for CO_2 conversion with 100% atom-utilization. Metal–organic frameworks are a kind of potential heterogeneous catalysts, however, high temperature, high pressure, and high-purity CO_2 are still required for the reaction. Here, we report two new Zn(II) imidazolate frameworks incoporating MoO_4^{2-} or WO_4^{2-} units, which can catalyse cycloaddition of CO_2 and epichlorohydrin at room temperature and atomospheric pressure, giving 95% yield after 24 h in pure CO_2 and 98% yield after 48 h in simulated flue gas (15% CO_2 + 85% N_2), respectively. For comparison, the analogic Zn(II) imidazolate framework MAF-6 without non-3d metal oxide units showed 71% and 33% yields under the same conditions, respectively. The insightful modulation mechanisms of the MoO_4^{2-} unit in optimizing the electronic structure of Zn(II) centre, facilitating the rate-determined ring opening process, and minimizing the reaction activation energy, were revealed by X-ray photoelectron spectroscopy, temperature programmed desorption and computational calculations.

CO_2 emission from the excessive use of fossil fuel has become one of the most serious global environmental problems [1–4]. Efficient capture and utilization of CO_2 is one of the keys to achieve the goal of carbon neutrality [5–13]. The cycloaddition of CO_2 and epoxide, as the key reaction to produce biodegradable polymers and electrolytes for lithium-ion battery, and featuring the atom-utilization efficiency of 100%, is one of the most efficient ways for CO_2 fixation [14–18]. In industry, homogeneous catalysts are prerequisite for this reaction so far, and many efforts have been devoted to developing high-performance heterogeneous catalysts [19–21]. If the catalyst have high activity at room temperature and low CO_2 concentration, the flue gases (*ca.* 15% CO_2) [22–25] could be directly used as the feedstock, which avoids the energy-consuming processes of CO_2 separation, transportation, pressurization, *etc.* [26–29].

Among numerous types of porous materials, metal–organic frameworks (MOFs) possess many advantages for heterogeneous catalysis including convenient synthesis and modification, well-defined active sites, and uniform pore structures [30,31]. Moreover, MOFs can supply some unique active structures which can be hardly constructed in other types of heterogeneous catalysts [32–34]. Even so, high temperature and/or high pressure are generally needed for CO_2 cycloaddition reactions, especially when low-concentration CO_2 is used as the reactant [35–37], which illustrates the relatively low activities of known MOF catalysts.

As a kind of famous MOFs with excellent stability and relatively low cost, metal azolate frameworks (MAFs), such as MAF-4/ZIF-8, demonstrate great advantages in adsorption, separation, sensing and more, but exhibit relatively low catalytic performances for CO_2 cycloaddition [17,38], indicating low acidity of the simple tetrahedral metal centres coordinated with nitrogen donors. Recent research revealed that high-valency non-3d metals are promising to modulate the electronic structures of catalytic active centres [39,40]. For example, $[Co_4(MoO_4)(eim)_6]$ (MAF-69-Co-Mo, Heim = 2-ethylimidazole) and $[Co_4(WO_4)(eim)_6]$ (MAF-69-Co-W) showed high electro-catalytic OER performances because the MoO_4^{2-} and WO_4^{2-} units can tailor the electronic structures of Co(II) centres [41]. In this work, we synthesized their zinc(II) analogues for high-performance CO_2 cycloaddition under ambient con-

* Corresponding authors.
E-mail addresses: hct@jxnu.edu.cn (C.-T. He), cxm@mail.sysu.edu.cn (X.-M. Chen).
[1] These authors contributed equally to this work.

https://doi.org/10.1016/j.cclet.2022.107814
1001-8417/

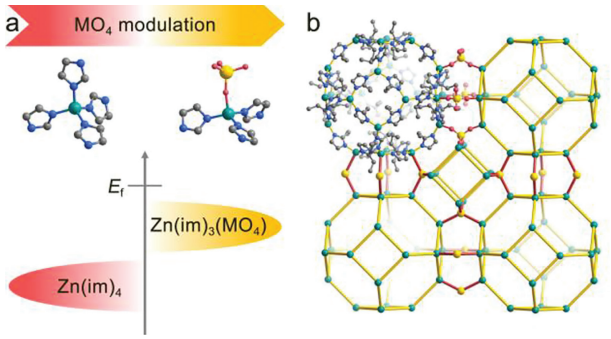

Fig. 1. (a) Schematic presentation of tailoring *d*-band electronic structure of Zn by MO_4 modulation. (b) Structure and topology of **1** and **2** (yellow: Mo or W; green: Zn; blue: N; grey: C; red: O).

dition using pure CO_2 and even simulated flue gas as the reaction source.

Considering that Zn(II)-based MOFs usually show higher activity than Co(II)-based ones for CO_2 cycloaddition reactions [42–44], two new MOFs, namely $[Zn_4(MoO_4)(eim)_6]$ (denoted as MAF-69-Zn-Mo or **1**) and $[Zn_4(WO_4)(eim)_6]$ (denoted as MAF-69-Zn-W or **2**), were synthesized according to the synthetic method for MAF-69-Co (Fig. 1a). Both single-crystal X-ray diffraction (SCXRD) and powder X-ray diffraction (PXRD) analyses confirmed that both **1** and **2** are isostructural with MAF-69-Co (Figs. 1b and 2a, Figs. S1 and S2, Table S1 in Supporting information). The Zn–N bond lengths in **1** are slightly shorter than those in **2**, implying that the electron-withdrawing effect of MoO_4^{2-} toward Zn(II) is stronger than that of WO_4^{2-}. This result could be further confirmed by Fourier transform infrared (FT-IR) spectra (Fig. S3 in Supporting information) [45]. To study the role of non-3d metal modulation effects, RHO-$[Zn(eim)_2]$ (MAF-6) [46], an analogue of zinc imidazolate, was also synthesized for comparison. PXRD confirmed the phase purity of all microcrystalline samples (Fig. S4 in Supporting information). Scanning electron microscope (SEM) showed particle sizes of *ca.* 630, 131 and 420 nm for **1**, **2** and MAF-6, respectively (Figs. 2b and c, Figs. S5–S8 in Supporting information).

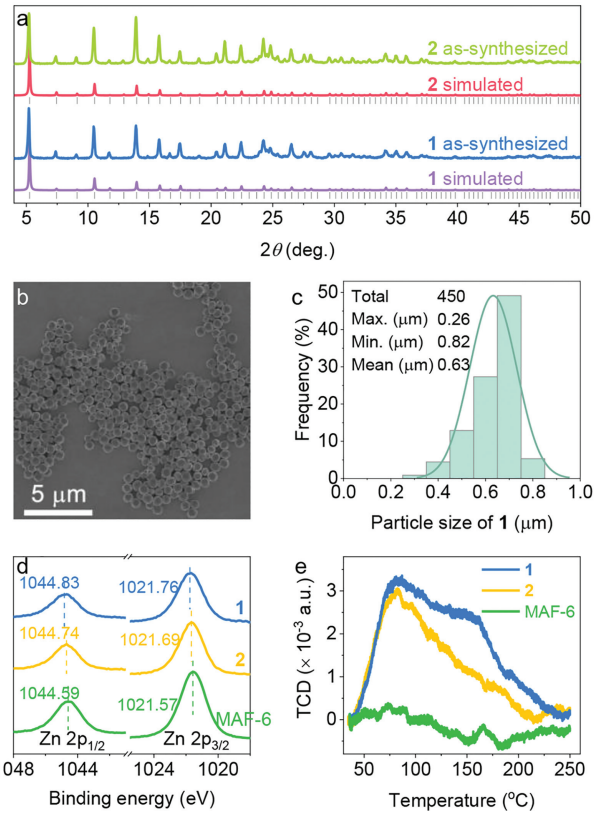

Fig. 2. (a) PXRD patterns. (b) SEM image and (c) particle size distribution of **1**. (d) High-resolution Zn 2p orbital XPS profiles. (e) NH_3-TPD.

Scheme 1. Catalytic cycloaddition reaction between ECH and CO_2.

Both **1** and **2** exhibited excellent thermal and chemical stabilities. Thermogravimetry and PXRD revealed that **1** and **2** can be stable up to at least 400 °C (Figs. S9-S11 in Supporting information). PXRD showed that **2** and **1** can be stable in water under pH 1−13 and pH 3−13 for at least one week, respectively (Figs. S12 and S13 in Supporting information). At 298 K and 1 atm (Fig. S14 in Supporting information), the CO_2 uptake of **1** (0.44 mmol/g) is higher than that of **2** (0.37 mmol/g), implying **1** exhibits stronger CO_2 affinity than **2** does, as their void volumes (**1**: 0.14 cm^3/g; **2**: 0.13 cm^3/g) are highly similar.

X-ray photoelectron spectroscopy (XPS) was employed to investigate the electronic structures of metal ions, which usually have crucial influence on the catalytic properties (Fig. 2d). In the high-resolution spectra of the 2p orbits of Zn, the orbital binding energies follow **1** (1044.8 and 1021.8 eV) > **2** (1044.7 and 1021.7 eV) > MAF-6 (1044.6 and 1021.6 eV), indicating that a stronger electron-withdrawing property of MO_4^{2-} and an increased charge density of Zn, consistent with the bond length results (Table S2 in Supporting information). Moreover, in the temperature programmed desorption curves of NH_3, the desorption temperatures and amounts follow **1** > **2** > MAF-6 (Fig. 2e), demonstrating a Lewis acidity sequence of **1** > **2** > MAF-6.

The CO_2 cycloaddition reaction with epichlorohydrin (ECH) as the reaction substrate and tetrabutylammonium bromide (TBAB) as a co-catalyst at ambient condition (Scheme 1) was employed as a model reaction to evaluate the enhanced catalytic activities of **1**. Through Proton nuclear magnetic resonance (^{1}H-NMR), the reaction process and the corresponding conversion can be determined. In Fig. 3a and Fig. S15 (Supporting information), compound **1** exhibits a 95% and 99% of ECH conversion ratio after 24 and 48 h in pure CO_2, respectively, and thus the reaction in pure CO_2 was fixed as 24 h in subsequent comparison. Notably, compound **1** represents a rare example that can efficiently catalyze CO_2 cycloaddition reactions at room temperature and ambient pressure and such high conversion is among the highest values for MOF catalysts at ambient condition (Table S3 in Supporting information) [17]. Besides, the conversions of ECH are found to be close to 0 when the TBAB was absent. The necessity of TBAB (nucleophilic Br^- as Lewis base to attack epoxide and open the ring) illustrates that

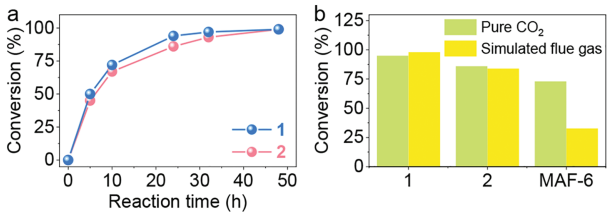

Fig. 3. (a) Reaction conversions of cycloaddition between CO_2 and ECH under ambient conditions catalyzed by **1** and **2**. (b) Comparison of catalytic efficiencies at ambient temperature and pressure of **1**, **2** and MAF-6 for CO_2 cycloaddition of ECH in pure CO_2 for 24 h and in simulated flue gas for 48 h, respectively.

these MAF catalysts only provide the metal sites as Lewis acid for the reaction (Fig. S16 in Supporting information). Expectedly, compound **1** showed high recyclability for the ECH-CO_2 cycloaddition reaction (Fig. S17 in Supporting information). After five reaction cycles, the conversion can still reach 97% in 24 h, and the recycled frameworks remained intact as verified by PXRD (Fig. S18 in Supporting information). In addition, the reactants were extended to other epoxides to further verify the catalytic activity of **1** (Table S4 in Supporting information). When the reactant was butylene oxide, the conversion ratio also can reach 94% after 24 h. Nevertheless, the conversion ratio gradually decreases for the bulkier epoxides, which may be attributed to the limitation of pore on the diffusion of large reactants.

The 24-h conversion of ECH in pure CO_2 catalyzed by **1**, **2** and MAF-6 were determined as 95%, 86% and 73%, respectively. And the corresponding turnover frequency (TOF) can be calculated as 19.8, 17.9 and 14.8 h^{-1}, respectively. Furthermore, it is known that the catalytic activities of MAF-4 and [Zn(cbIm)$_2$] (ZIF-95, HcbIm = 5-chlorobenzimidazole) are based on coordinated defects on the crystal surface, *i.e.*, Zn ion and terminal coordinated hydroxide, whose acidity and basicity are weak so that their performances are low even with TBAB [47,48]. In principle, the MO_4^{2-} units in **1** and **2** not only increase the acidity of Zn but also decrease the basicity of the terminal hydroxide group. Therefore, they exhibit enhanced catalytic activity toward CO_2 cycloaddition compared with the simple binary Zn-imidazolate framework. Moreover, the high catalytic activity of **1** was highlighted by using simulated flue gas as the CO_2 source. Under such a low CO_2 concentration, the conversion ratio still reached 48% after 24 h and 98% after 48 h (Fig. 3b and Fig. S19 in Supporting information), which are among the highest for MOF catalysts at similar conditions (Table S5 in Supporting information) [49,50]. As a comparison, the 48-h conversion ratios merely reach 84% and 33% for **2** and MAF-6, respectively, also verifying the catalytic activity order of **1** > **2** > MAF-6.

In order to understand the different catalytic performances of zinc imidazolate centres, we also carried out computational simulations by density functional theory (DFT). We initially calculated the electrostatic potential (ESP) charges of zinc atoms, giving the $ESP_{\mathbf{1}}$ of 0.498 and $ESP_{MAF\text{-}6}$ of 0.326, respectively, which agree well with the experimental results of XPS and TPD (**1** with more positively charged zinc centre). The partial density of states (PDOS) of *d* orbital on the active metal sites, was shown in Fig. S20 (Supporting information). The *d*-orbital centre of **1** was remarkably shifted toward the Fermi level compared with that of MAF-6, demonstrating the electronic modulation effect of MoO_4^{2-} unit toward zinc centre. Furthermore, according to Park *et al.* [51], the whole reaction process contains ring opening of the three-membered ring and CO_2 insertion to form carbonate ester (Fig. 4 and Fig. S21 in Supporting information), involving two corresponding transient states (TS). According to the calculation results, **1** exhibits a more mitigated energy change thermodynamically during the reaction process, suggesting the optimal electronic structure of Zn centre of **1**. Moreover, the rate determined step (RDE) can be confirmed as the ring opening reaction, during which the α-C atom of ECH is attacked by the Br^- of TBAB to form the bromo-substituted alkoxide intermediate (TS1), also verifying the necessity of co-catalysts. For MAF-6, the activation energy of TS1 was 116.3 kJ/mol, whereas that of **1** was dramatically decreased to 36.1 kJ/mol, being consistent with the experimental activities. Alternative to MAF-6, the reaction activation energy of TS1 is probably reduced by the unique hydrogen bonding interaction (C-H···O = 2.39 Å) between the proton on α-C atom of ECH and the coordinated O atom on Zn centre in **1** (Fig. S22 in Supporting information). These results indicate that the insight of MoO_4^{2-} unit on boosting CO_2 cycloaddition includes optimizing the electronic structure of Zn centre, facilitating the rate-determined ring opening process and minimizing the reaction activation energy.

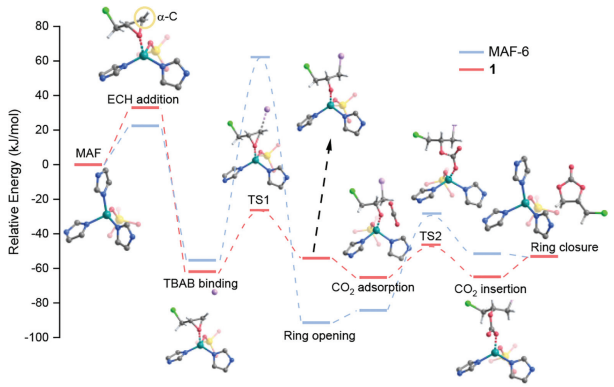

Fig. 4. DFT-derived energy profiles of the proposed ECH cycloaddition process catalyzed by **1** and MAF-6 with corresponding structures of the active sites and intermediates of **1** during reaction. The capping ligand, ethyl group and hydrogen atoms are omitted for clarity (yellow: Mo; green: Zn; blue: N; grey: C; red: O; light green: Cl; white: H; pink: Br).

In summary, two non-3d metal integrated zinc imidazolate frameworks with high thermal and chemical stabilities were successfully synthesized. Spectroscopic characterizations and DFT calculations revealed that the non-3d metal oxides MO_4^{2-} units can effectively tailor the electronic structure of Zn(II) ion, resulting that **1** exhibited the highest catalytic activity for cycloaddition between CO_2 and ECH under room temperature with low concentration CO_2 or simulated flue gas, which is very important for practical application in reducing the energy consumption. Our findings provide a new thought to the design of coordination catalysts for efficient CO_2 conversion.

Declaration of competing interest

The authors declare that they have no known competing financial interests or personal relationships that could have appeared to influence the work reported in this paper.

Acknowledgments

This work was supported by the National Natural Science Foundation of China (Nos. 22090061, 21731007, 21890380 and 22161021) and the Guangdong Pearl River Talents Program (No. 2017BT01C161). C.-T. He acknowledges the support of Jiangxi Province (No. jxsq2018106041). Prof. Jie-Peng Zhang is appreciated for his helpful suggestions and discussion.

Supplementary materials

Supplementary material associated with this article can be found, in the online version, at doi:10.1016/j.cclet.2022.107814.

References

[1] L. Yang, C. Zhang, X. Yu, et al., Natl. Sci. Rev. 8 (2021) nwab104.
[2] X. Ren, S. Liu, H. Li, et al., Sci. China Chem. 63 (2020) 1727–1733.
[3] S.C. Peter, ACS Energy Lett. 3 (2018) 1557–1561.
[4] J. Liu, C. Chen, K. Zhang, L. Zhang, Chin. Chem. Lett. 32 (2021) 649–659.
[5] M. Ding, R.W. Flaig, H.L. Jiang, O.M. Yaghi, Chem. Soc. Rev. 48 (2019) 2783–2828.
[6] W. Gao, S. Liang, R. Wang, et al., Chem. Soc. Rev. 49 (2020) 8584–8686.
[7] D.D. Zhou, X.W. Zhang, Z.W. Mo, et al., Energy Chem. 1 (2019) 100016.
[8] Q. Wang, H. Pfeiffer, R. Amal, D. O'Hare, React. Chem. Eng. 7 (2022) 487–489.
[9] K. Jiang, P. Ashworth, S. Zhang, et al., Renew. Sust. Energy Rev. 119 (2020) 109601.
[10] Y. Shi, J. Zhao, H. Xu, S.L. Hou, B. Zhao, Sci. China Chem. 64 (2021) 1316–1322.
[11] N. Wang, R.K. Miao, G. Lee, et al., SmartMat 2 (2021) 12–16.

[12] C. Yang, Z. Gao, D. Wang, et al., Sci. China Mater. 65 (2022) 155–162.
[13] X. Dong, Z. Xin, D. He, et al., Chin. Chem. Lett. 34 (2023) 107459.
[14] M. Liu, X. Wang, Y. Jiang, J. Sun, M. Arai, Catal. Rev. 61 (2019) 214–269.
[15] G. Yuan, Y. Lei, X. Meng, et al., Inorg. Chem. Front. 9 (2022) 1208–1216.
[16] J. Hu, H. Liu, B. Han, Sci. China Chem. 61 (2018) 1486–1493.
[17] J. Liang, Y.B. Huang, R. Cao, Coord. Chem. Rev. 378 (2019) 32–65.
[18] H. Hu, D. Zhang, H. Liu, et al., Chin. Chem. Lett. 32 (2021) 557–560.
[19] G.N. Bondarenko, E.G. Dvurechenskaya, O.G. Ganina, F. Alonso, I.P. Beletskaya, Appl. Catal. B: Environ. 254 (2019) 380–390.
[20] A. Rehman, V.C. Eze, M.F.M.G. Resul, A. Harvey, J. Energy Chem. 37 (2019) 35–42.
[21] L.G. Ding, B.J. Yao, F. Li, et al., J. Mater. Chem. A 7 (2019) 4689–4698.
[22] T.M. McDonald, W.R. Lee, J.A. Mason, et al., J. Am. Chem. Soc. 134 (2012) 7056–7065.
[23] O.H. Animasahun, M.N. Khan, C.J. Peters, Mol. Phys. 116 (2018) 3434–3445.
[24] D. Lv, J. Chen, K. Yang, et al., Chem. Eng. J. 375 (2019) 122074.
[25] H. Lv, R. Sa, P. Li, et al., Sci. China Chem. 63 (2020) 1289–1294.
[26] Y. Cheng, J. Hou, P. Kang, ACS Energy Lett. 6 (2021) 3352–3358.
[27] J. Chen, H. Li, M. Zhong, Q. Yang, Green Chem. 18 (2016) 6493–6500.
[28] H. Zhong, J. Gao, R. Sa, et al., ChemSusChem 13 (2020) 6323–6329.
[29] F. Duan, X. Liu, D. Qu, B. Li, L. Wu, CCS Chem. 3 (2021) 2676–2687.
[30] C. Duan, K. Liang, J. Lin, et al., Sci. China Mater. 65 (2022) 298–320.
[31] G. Si, X. Kong, T. He, et al., Chin. Chem. Lett. 32 (2021) 918–922.
[32] J. Liang, Y.Q. Xie, X.S. Wang, et al., Chem. Commun. 54 (2018) 342–345.
[33] Y. Peng, W. Yang, Sci. China Chem. 62 (2019) 1561–1575.
[34] X.J. Hu, Z.X. Li, H. Xue, et al., CCS Chem. 2 (2020) 616–622.
[35] B. Ugale, S. Kumar, T.J. Dhilip Kumar, C.M. Nagaraja, Inorg. Chem. 58 (2019) 3925–3936.
[36] W. Zhang, F. Ma, L. Ma, Y. Zhou, J. Wang, ChemSusChem 13 (2020) 341–350.
[37] S.H. Kim, R. Babu, D.W. Kim, W. Lee, D.W. Park, Chin. J. Catal. 39 (2018) 1311–1319.
[38] C.M. Miralda, E.E. Macias, M. Zhu, P. Ratnasamy, M.A. Carreon, ACS Catal. 2 (2012) 180–183.
[39] B. Zhang, L. Wang, Z. Cao, et al., Nat. Catal. 3 (2020) 985–992.
[40] F. Wang, Z.S. Liu, H. Yang, Y.X. Tan, J. Zhang, Angew. Chem. Int. Ed. 50 (2011) 450–453.
[41] Y.T. Xu, Z.M. Ye, J.W. Ye, et al., Angew. Chem. Int. Ed. 58 (2019) 139–143.
[42] B. Mousavi, S. Chaemchuen, B. Moosavi, et al., Chem. Open. 6 (2017) 674–680.
[43] J. Sirijaraensre, New J. Chem. 43 (2019) 11692–11700.
[44] R. Zou, P.Z. Li, Y.F. Zeng, et al., Small 12 (2016) 2334–2343.
[45] E. Shamsaei, Z.X. Low, X. Lin, et al., Chem. Commun. 51 (2015) 11474–11477.
[46] X.C. Huang, Y.Y. Lin, J.P. Zhang, X.M. Chen, Angew. Chem. Int. Ed. 45 (2006) 1557–1559.
[47] K.M. Bhin, J. Tharun, K.R. Roshan, et al., J. CO_2 Util. 17 (2017) 112–118.
[48] R.R. Kuruppathparambil, R. Babu, H.M. Jeong, et al., Green Chem. 18 (2016) 6349–6356.
[49] R. Das, D. Muthukumar, R.S. Pillai, C.M. Nagaraja, Chem. Eur. J. 26 (2020) 17445–17454.
[50] J. Gu, X. Sun, X. Liu, et al., Inorg. Chem. Front. 7 (2020) 4517–4526.
[51] A.C. Kathalikkattil, R. Babu, R.K. Roshan, et al., J. Mater. Chem. A 3 (2015) 22636–22647.